Nabladot Analysis of Hybrid Theories in International Relations

Claudio Cioffi-Revilla

> Suffice it to remember what Kant asserted;
> that progress in every science is measured in
> terms of its use of mathematics. (Gori 2004, 44)

1. Introduction

International relations investigates a vast universe of political phenomena, most of it constituted by a mix of continuity and discreteness. The duration of diplomatic relations among countries, of peace between states, of international treaties, and of global international regimes in diverse policy domains are continuous variables; as are distance between capitals, speed of great power transitions, and probabilities associated with all international events. By contrast, the formal composition of a country's diplomatic organization, of alliances, governmental and nongovernmental international organizations, as well as the requisites of effective deterrence and other extant policies, are discrete variables. Time, space, territories, and emotions are generally continuous, but with discrete features such as barriers, thresholds, empty spaces, layers, and boundaries, which are discrete. This hybrid texture of continuity and discreteness—i.e., "concreteness," meaning simultaneously *continuous and discrete*—is ubiquitous, consequential, and fundamental in international relations, as reflected by theory and research across the discipline (and throughout social science in general).

Research and analysis of hybrid theories of international relations is conducted through mathematical tools from the infinitesimal calculus of Newton and Leibniz and discrete calculus developed in recent decades. Both are needed to understand real-world international phenomena that are otherwise not knowable through purely historical or narrative discussions (Gillespie 1976; Kline 1985; Cioffi 1998). Until recently, however, infinitesimal and discrete calculi

Claudio Cioffi-Revilla, George Mason University, United States, ccioffi@gmu.edu, 0000-0001-6445-9433
Referee List (DOI 10.36253/fup_referee_list)
FUP Best Practice in Scholarly Publishing (DOI 10.36253/fup_best_practice)
Claudio Cioffi-Revilla, *Nabladot Analysis of Hybrid Theories in International Relations*, © Author(s), CC BY 4.0, DOI 10.36253/978-88-5518-595-0.04, in Fulvio Attinà, Luciano Bozzo, Marco Cesa, Sonia Lucarelli (edited by), *Eirene e Atena. Studi di politica internazionale in onore di Umberto Gori*, pp. 31-53, 2022, published by Firenze University Press, ISBN 978-88-5518-595-0, DOI 10.36253/978-88-5518-595-0

have remained largely disjoint. Here we demonstrate a new unified calculus of hybrid functions with novel applications to a small, albeit representative and convincing sample of international relations theories. As a scientific system for exploration and discovery, this new analysis uncovers novel, significant, and often surprising features and properties of international phenomena that are otherwise inaccessible and, therefore, remain unknown, through earlier approaches. This investigation demonstrates results through formal mathematical and computational analysis supported by visual analytics, similar to the use of alternative "diagnostic imagery" in medical analyses or different ensembles of observational instruments in scientific research.

The next section provides examples of hybrid phenomena in international relations, followed by a section on the methodology of nabladot calculus for unified hybrid analysis. The fourth section investigates three specific cases that demonstrate hybrid analysis applied to international phenomena. Since our interest is substantive (as in all applied mathematics), we focus mainly on significant features of international political phenomena rather than purely mathematical themes. The last section provides concluding remarks.

2. Hybridity and hybrid functions in international relations theories

Continuity and discreteness—ontological hybridity—are present in the following international phenomena and their respective theoretical *explanans*:

Peace and other compound international events. All international events—e.g, political integration, alliance formation, conditions for peace, success of international regimes, deterrence requirements, nuclear proliferation containment, and international communication—are *compound events*, in the sense of probability theory, because they are always caused by several (i.e., more than one) conjunctive events (Bittinger and Crown 1982; Bruschi 1990; Goertz and Starr 2003). Consequently, the probability of an international event is a function of some discrete number of causal conditions required for its occurrence and a continuous value of probability associated with each causal event (Wohlstetter 1968; Cioffi 1998, chs. 5–7).

Growth of great powers or empires (Taagepera's law). At the actor-level of analysis, as an empire expands from some initially small size up to its maximum size, its growth is governed by a logistic function, where time is strictly continuous but the rate of polity expansion is discrete—by chunks of territory (provinces, other administrative units, conquered territories bound by natural barriers, fortifications, and other limiting factors (Taagepera 1968; 1978; 1979).

Wright-Snyder crisis theory of war. An inter-state war *never* "comes out of the blue" but, rather, originates from a prior crisis (a crisis being a metastable phase-transition, in complexity-theoretic terminology). The crisis- and bargaining-based theory explains the onset of interstate war as the violent escalation outcome of a process with multiple outcomes, war amongst them. In this theory, the probability of war in a given epoch is a function of some discrete number of

crises during the epoch and the probability of escalation to war in each crisis (Wright 1942, 1271–76, fn. 38; Deutsch 1978; Snyder and Diesing 1977, 13–5 *et passim*; Cioffi 1998, 160–63).

Loss-of-power gradient. At the relational or meso-level of analysis, continuity and discreteness over accessible time and space have mixed effects on the exercise of power ("power projection") at distances away from home base. While the rate of decay can assume positive continuous values, distance from home base is discrete (determined by military bases, supply chains, and other discrete systems and networks), so the overall function of these two quantities is hybrid (Boulding 1962; Wohlstetter 1968).

Size of war alliances (Horvath-Foster law). The frequency of war alliances in politico-military history shows a pattern that decreases with the size of the alliance. Informally, there have been many small war alliances, very few large ones, and an intermediate number in between (Horvath & Foster 1963). This is known as a discrete Yule-Simon distribution with continuous parameter and is symptomatic of complex systems and generative processes that are far from equilibrium; otherwise, the size distribution of war alliances would be normal or Gaussian (as in the height or weight of persons).

Warfare and international systemic polarity (Midlarsky's law). At the systemic or macro-level of analysis, the annual frequency of warfare in the international system varies in proportion to the number of great powers in the system, known as polarity. However, the frequency of wars increases with marginally decreasing increments in systemic polarity, so this too is a hybrid, nonlinear relationship (Midlarsky 1974).

Numerous other instances of international phenomena and corresponding theoretical explanations exist in international relations. Here we shall use instances 1, 3, and 6 to demonstrate how and why they are investigated through nabladot analysis, as described in the next section.

3. Mathematical methods for hybrid functions in IR

Consider a *hybrid function*, $Z = \varphi(X, Y)$, such that $(X, Y) \to Z \in \mathcal{R}$, where X and Y are real-valued continuous and discrete *independent variables*, respectively.[1] Nabladot analysis of a hybrid function $\varphi(X, Y)$ begins by (1) clarifying the hybrid domain of φ, specifically its substantive subdomains $x \in X$ and $y \in Y$ along each independent variable—such subdomain always being a bounded subspace of some broader mathematical domain and then, (2) specifying each variable's unit of measurement. This initial phase of analysis normally includes various graphs of φ for visual analysis, which are typically 2D or 3D

[1] We shall restrict attention to *scalar* hybrid functions, although *vector* hybrid functions also arise in nabladot analysis of scalar functions, as we shall see later in section 4, just as they do in classical analysis. Surveys of mathematical methods in political science and international relations include Cioffi (1979), Ashford et al. (1993), Moore and Siegel (2013).

surface graphs and contour plots of the hybrid function under investigation. As we shall see, ensembles of these interrelated graphs constitute theoretical landscapes—complete with singularities, basins, escarpments, canyons, and other topographic features—that provide sometimes surprisingly faceted or nuanced explanations and deeper understanding of each of the hybrid functions.

The next phase—and first properly analytical step in theoretical analysis—is to closely examine the causal effect of each independent variable on the dependent variable of interest, which is how the emergent field (dependent variable Z) is generated by the hybrid domain—given that φ maps the former (causes) onto the latter (effects). This consists of two steps that examine absolute and standardized effects, respectively. First, the first-order derivative and first-order difference of hybrid function are separately calculated, graphed, and examined, to understand absolute variations with respect to changes in X (continuous independent variable) and Y (discrete). This phase maintains the original units of measurement corresponding to each variable, since derivatives and differences are simple rates of change.

Second, the point elasticity and the arc elasticity of φ, denoted by η_x and η_y, respectively, are calculated to understand how patterns of variation in percentage change in each independent variable compare *independent of units of measurement* (which is what elasticity operators $\eta_x(Z)$ and $\eta_y(Z)$ are designed to investigate).[2] Additional graphs and visual analytics are used as well to better understand the structure and effects of elasticities—and add to the theoretical landscape of each hybrid function. This second phase results in transformed standardized dimensional space without units of measurements, making all independent variables and their direct effect on the dependent variable directly comparable. These results lead to one or more dominance principles, which are law-like statements that specify which independent variable has greatest causal effect on the dependent variable of the hybrid function—a fundamental property not always obvious from simple inspection of the hybrid function under investigation.

The analytical process thus far has focused on scalar properties of the IR hybrid function under investigation. The first nabladot operation is to calculate the hybrid gradient of Z to discover the magnitude *and* direction of changes in Z as a function of changes in X and Y. The result of applying the nabladot operator (a vector operator) to scalar hybrid function φ is a hybrid vector function $\mathbf{\Phi} = \nabla\varphi$ with x- and y-components. The hybrid gradient in two dimensions is the scalar vector product calculated using the new *nabladot vector operator* ∇ (note the dot within the nabla symbol), which is defined as follows:

$$\nabla\varphi \equiv \partial_x\varphi\ \mathbf{i} + \Delta_y\varphi\ \mathbf{j}, \tag{1}$$

[2] Economists call this "comparative statics," a phrase we shall *not* use here because *time* can be an independent variable of interest (e.g., as in Taagepera's law of empires) which—by definition—is not static.

where, by convention, **i** and **j** denote unit vectors along *x*- and *y*-dimensions, respectively, and ∂_x and Δ_y denote the first-order derivative and first-order difference with respect to *X* and *Y* (Cioffi 2014; 2017; 2019; 2020; 2020).[3] Note that the resulting nabladot gradient of hybrid function φ is a striated vector field with a first-order partial derivative component along the *x*-axis (continuous) and a first-order partial difference component along the *y*-axis (discrete), hence the striation of the vector field's topology.[4]

The absolute and standardized norms of the hybrid gradient $\nabla\varphi$ are calculated next, along with corresponding graphs for investigating the resulting vector field. Each pair of plots for a vector field and corresponding norm should use identical domains to facilitate understanding through comparative analysis. Cardinal directions (N, E, S, W) are used for simple orientation in graphs. Other hybrid operations of nabladot calculus equivalent to the divergence, curl, Laplacian, Hessian, and Jacobian are subsequently calculated to shed additional (and usually new) light on the original function $Z = \varphi(X, Y)$ through the medium of nabladot operators, each supported by additional graphic analyses.

The main results of nabladot analysis shed new light on fundamental, real-world, substantive properties and features of the original hybrid function under investigation, features that remain hidden or inaccessible through other forms of analysis. Each main formal expression is accompanied by an interpretation in plain English, although this is not always possible without some loss of precision or clarity. Some results can be somewhat complicated nonlinear functions that do not further simplify; we prefer them that way rather than introducing artificial approximations which may be simpler but unrealistic or unnatural objects, unlike real IR phenomena. In most cases an ensemble of images and visual analytics (Thomas and Cook 2005; Wellin 2013) of complicated functions can add significant clarity.

Among the most important substantive (and testable) results from nabladot analysis are the dominance principles mentioned above—they explain which independent variable has dominant effect on the dependent variable, a major theoretical (and arguably policy) question impossible to answer *ex ante*—as well as other characteristic phenomena of interest (e.g., discrete striations, inflection or "tipping" points, asymptotes and other singularities, constant or invariant subfields, and others) revealed by geometric and topological infor-

[3] IR scholars rarely consider the presence of vectors in international relations, other than metaphorically. This analysis demonstrates the rigorous analysis of vectors and vector fields in IR using formal methods from nabladot calculus, as in the next section. To contain notation, we shall use **i** and **j** to denote unit vectors along continuous and discrete dimensions, respectively, rather than create new unit vectors for each variable.

[4] Use of the partial derivative with respect to *Y* (a discrete variable) instead of the partial difference—which is often used in approximations—produces a measurable error that varies in magnitude depending on the structure of φ and values of *Y*. Measurable discrepancies between the two operators (nabladot and classical nabla) are demonstrable but beyond the present scope due to space limitations (Cioffi 2021).

mation. In addition, interesting scalar and vector fields of φ become accessible to direct investigation through formal tools of nabladot calculus and analysis. A novel and valuable feature of this approach is that nabladot calculus provides exact results in analytical investigations where the classical infinitesimal calculus of hybrid IR functions would provide approximations with errors over the discrete domain of independent variable(s).

4. Applications to areas of international relations

Here we shall investigate three illustrative cases of IR theories and research areas—numbered 1, 3, and 6 in section 2—where hybrid functions play a central role in describing and explaining political phenomena. The scientific purpose is to deepen our understanding and provide foundations for more advanced analysis. Each "case study" follows the analytical procedure just outlined in section 3.

4.1 Case 1: Peace and other international events

All international events in the real world are "compound" because they are always produced by necessary conditions specific to the event. Such causal necessity is universal—a fundamental axiom in all domains of international relations theory. For example, consider the event defined by the following expression:

$$\mathbb{S} \equiv \text{"a state of stable peace exists between two countries."} \qquad (2)$$

This is a compound event because $\mathbb{S}$ requires the following set of causally necessary conditions, each of which constitutes an event by itself:

1. Neither state will pursue issues deemed as highly threatening to the other, as opposed to acting completely oblivious or independently of extant foreign interests.
2. Each state may prefer to negotiate over colliding interests, before escalating to war.
3. When states do negotiate, they may—depending on conditions—find a nonviolent resolution.

The universal existence of such necessary conditions makes $\mathbb{S}$ a compound event, by definition.

Specifically, every international event $\mathbb{E}$ is produced by causal *conjunction* (operator $\wedge$) of necessary events—i.e., set-theoretic *intersection* (operator $\cap$) or Boolean logic *product* (operator AND). Let $\{\mathbb{X}_i\}_{i=1}^{n}$ denote a set of *N* necessary events that produce $\mathbb{E}$. Causal production of $\mathbb{E}$ is specified by an *event function*, $\Psi_{\mathbb{E}} : \{\mathbb{X}_i\} \rightarrow \mathbb{E}$, which maps necessary events in $\{\mathbb{X}_i\}$ onto $\mathbb{E}$ using causal conjunctions. The number of events in a compound event (its "size" or "conjunctivity"), is called *cardinality*, $|\mathbb{E}| = \{1, 2, 3, \cdots, n\} \subset \mathcal{N}$, which is always a natural number (positive integer), so cardinality (or "event size") is always a discrete

variable. For example, compound event $\mathbb{S}$ in equation 2 ("a size 3 event") is first-order conjunctive with respect to its three causally necessary events.[5] Formally, we can summarize these ideas through the following expression:

$$\mathbb{E} \Leftarrow \Psi(\mathbb{E}) = \mathbb{E}_1 \wedge \mathbb{E}_2 \wedge \cdots \wedge \mathbb{E}_n = \bigwedge_{i=1}^{n} \mathbb{E}_i. \tag{3}$$

Next, an international event $\mathbb{E}$ has probability $\Pr(\mathbb{E})$ that is determined by the naturally uncertain occurrence of necessary conditions—a type of causation known as *probabilistic causality* (Salmon 1980; Suppes 1984; Eels 1991). Based on Kolmogorov's (1933) fundamental theorem of compound events, the joint probability E of compound event $\mathbb{E}$ is given by the following expression:

$$\Pr(\mathbb{E}) = \Pr(\mathbb{E}_1) \cdot \Pr(\mathbb{E}_2) \cdot \ldots \cdot \Pr(\mathbb{E}_n) = \prod_{i=1}^{n} \Pr(\mathbb{E}_i), \tag{4}$$

where events $\mathbb{E}_i$ are independent; when they are *not* independent, *conditional probabilities* are used and, by Kolmogorov's theorem, they still multiply. Letting $\Pr(\mathbb{E}) = E$ and $\Pr(\mathbb{E}_i) = p_i$, since all probabilities are continuous variables (i.e., E and p_i are variables, not events), we can rewrite equation (4) in simpler notation:

$$E = p_1 \cdot p_2 \cdot \ldots \cdot p_n = \prod_{i=1}^{n} p_i \tag{5}$$

$$= P^N, \tag{6}$$

where P is the probability of causal events and $N \equiv |\mathbb{E}|$ is the cardinality or event size. Note that equation 6 is a *hybrid function*, because probability is continuous on the unit interval of real numbers [0,1]—which lies between (and includes) impossibility ($E = 0$) and certainty ($E = 1.0$)—while event size is always a discrete or natural number (of necessary conditions).

The politically relevant domain of interest—in this case—is bound by $0 \leq P \leq 1$ and $2 \leq N \lessapprox 20$ along causal probability and size dimensions in the hybrid (p, n) domain. Specifically, equation 6 is a hybrid function linearly dependent in P and exponentially in N, so this means that changes in either variables will cause different political effects on the probability of an event.

The 3D surface graph of equation 6 is in Figure 1a, which shows values of the probability E of an international event rising through a steep escarpment as causal probability P increases and cardinality N decreases. The contour plot

[5] An event function Ψ is also called *indicator function*, *structure function*, or *production function*, in areas of mathematics, engineering, and economics, respectively.

in Figure 1b shows the graph looking straight down, which highlights the ample basin floor where causal probability is very low ($0 \leq P \lessapprox \leq 0.9$), flanked by the steep north-south escarpment along the east edge as $P \rightarrow 1.0$.

Note that change caused by each variable differs, as shown in Figures 1c through f. Calculating the partial derivative and partial difference of *E* with respect to *P* and *N*, respectively:

$$\partial_p E = NP^{N-1} \quad \text{(for } P\text{'s effect on } E\text{, in Figures 1c and d)} \quad (7)$$

$$\Delta_n E = P^{N+1} - P^N \quad \text{(for } N\text{'s effect on } E\text{, in Figures 1e and f).} \quad (8)$$

We see immediately that changes in causal probability *P* and event size *N* have different effects on the probability of an international event *E*, besides the trivial observation that *any* change on either variable has *some* effect on *E* (since $\partial_p E \neq 0$ and $\Delta_N E \neq 0$, per equations 7-8). To wit:

Opposite political effects. Whereas change in causal probability *P* has proportional or positive effect on *E*, change in event size *N* has an opposite effect. This is shown by the purple deep bottom in Figure 1c versus the high red plateau in Figure 1e; both features observed over approximately the same underlying (*p*, *n*)-domain.

First- and second-order effects. Whereas the contour plot of $E(P, N)$ shows strictly concave isocontours (Figure 1b), the contours of the derivative $\partial_p E$ (Figure 1d) also show a convex, mild spur protruding on the southwestern wall of the escarpment, near $p = 0.75$ (third contour, between green and blue elevations), which means more complex change for small-size events. This is a second-order effect and not at all intuitive from the basic model (equation 6 and Figures 1a and b).

Second-order effects caused by changes in event size. The graphs of the change in *E* with respect to event size, $\Delta_n E$ (equation 8 and Figures 1e and f), show a pronounced ravine or canyon along the north-south direction dropping into a deep precipice at relatively high values of *P* as $N \rightarrow 2$. Interestingly, in this case all the isolines have mixed concavity (low *P*) and convexity (higher *P* values), which is another second-order effect.

Geometrically opposite extrema. The extreme high range of $\partial_p E$ in Figures 1c and d and the extreme low range of $\Delta_n E$ in Figures 1e and f have opposite (or inverse) geometries with some common similarities: the former rises from a flat basin to an escarpment while the latter drops from a large plateau toward a deepening canyon that dives into a deep well. Both features are indicative of major political effects on event probability *E* caused by underlying changes in causal probabilities *P* and event size *N*.

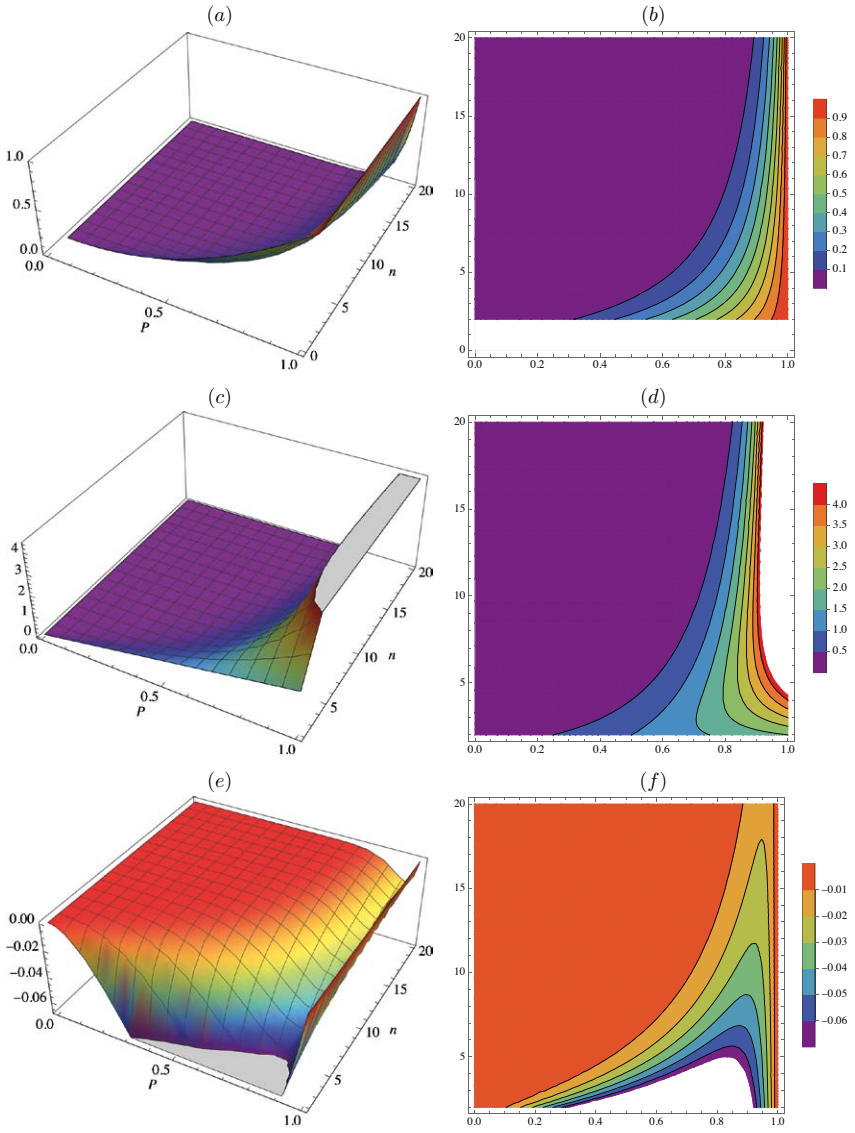

Figure 1. Probability of an international event $E(P, N)$ as a hybrid function of the probability P of N necessary conditions for its occurrence. (a) 3D surface of hybrid function $E = P^N$; (b) contour plot of (a); (c) 3D surface of $\partial_p E$, the first-order partial derivative of $E(P, N)$ with respect to P; (d) contour plot of (c); (e) 3D surface of $\Delta_n E$, the first-order partial difference of $E(P, N)$ with respect to N; (f) contour plot of (e).

These first insights begin to shed light on the nature of international events as a function of their necessary conditions. However, causal probability *P* and event size *N* are measured in different units (probability and number of events, respectively), so absolute rates of change (equations 7 and 8) fail to explain which variable has dominant effect on *E*. To solve this problem we obtain and analyze *standardized* (or percentage) rates of change in *E* with respect to *P* and *N* (called elasticities), as in Figure 2. Calculating the point elasticity and the arc elasticity of *E* with respect to *P* and *N*, respectively:

$$\eta_p E = N \qquad \text{(for } P\text{'s percentage effect on } E\text{, in Figures 1c and d)} \quad (9)$$
$$\eta_n E = (P-1)N \quad \text{(for } N\text{'s percentage effect on } E\text{, in Figures 1e and f).} \quad (10)$$

We see immediately that these standardized effects on *E* are very different from the earlier absolute, unit-based effects (equations 7 and 8).

The point elasticity—percentage change in the probability of an international event with respect to percentage change in *P*—is constant, as in Figures 2a and b, meaning that a percentage variation in probability of an international event *E* relative to a percentage variation in causal probability *P* is determined solely by event size *N* and is independent of *P*. By contrast, arc elasticity—percentage change in *E* with respect to percentage change in *N*—is linear in both independent variables, as in Figures 2c and d, resulting in a nonlinear scalar field as evidenced by the contour plot.

Comparing the two elasticities (equations 9 and 10) answers the universal question concerning which of the two causal variables has the dominant or greater effect on the probability of an international event. Since $N>(P–1)N$, this means that point elasticity η_p is greater than the arc elasticity η_n. Therefore, *E* is more sensitive to change in *P* (probability of necessary causal events) than to change in cardinality *N*—a result that may be called *dominance principle for international events*.

Although their effects differ, in reality both variables have joint, concurrent effects on international events. The joint effects of *P* and *N* on *E* can be better understood by calculating the gradient of *E* with respect to both variables using the nabladot operator, as follows:

$$\nabla E = \partial_p P^N \mathbf{i} + \Delta_n P^N \mathbf{j} \quad (11)$$
$$= N P^{(N-1)}\ \mathbf{i} + (P-1)P^N\ \mathbf{j}, \quad (12)$$

which is a two-dimensional vector function $\mathbf{E} = \Psi(P, N)$. The emergent vector field of this hybrid gradient is in Figure 2e and corresponding vector magnitude or norm $|\mathbf{E}|(P, N)$, which is a scalar function, is shown in Figure 2f. We see immediately that norm $|\mathbf{E}|$ is very similar to $\partial_p E$ in Figures 1e and d, which is not an intuitive result or obvious insight that could be obtained from casual comparison between the two dissimilar equations for the arc elasticity (equation 8) and the magnitude of **E**.

This concludes the first analysis of our three "case studies." The next two are presented in slightly abbreviated form to omit some procedural repetitions while

maintaining the method outlined in section 3. Analysis of the probability of international events in this first case leads us to investigate the probability of war onset—a special class of international event of fundamental historical significance since early antiquity and of theoretical interest (at least) since Thucydides—in the next section.

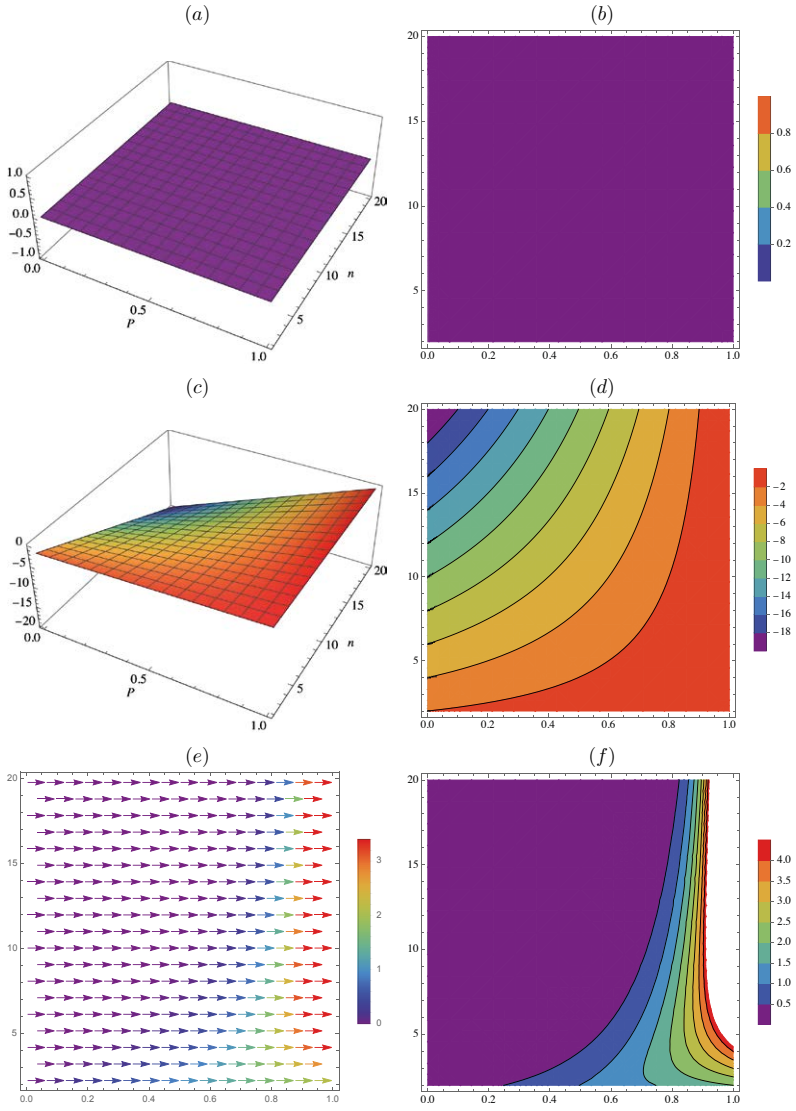

Figure 2. Elasticities and gradient of the probability of an international event E. (a) 3D surface of point elasticity $\eta_p(E)$ respect to causal probability P; (b) contour plot of (a); (c) 3D surface of arc elasticity η_n(E) with respect to number of necessary conditions N; (d) contour plot of (c); (e) vector field of the dot-gradient vector function ∇E; (f) contour plot of (e).

4.2 Case 2: Crisis dynamics and onset of war

Explaining the outbreak of international war as caused by a prior crisis escalation process—which includes challenging and resistance moves, bargaining, signaling, and other events, as opposed to some other causal mechanism—was first proposed by Quincy Wright (Wright 1942, 1271, fn. 38) and later extended and generalized by Glenn H. Snyder (Snyder Diesing 1977, 13–7 et *passim*). The frame of reference here is the inter-state relational level of analysis and the specific *explanandum* is the probability W of a state being at war over a period of time, called an epoch in probability theory.[6] During an epoch a country experiences a number C of crises (defined as episodes during which hostilities may occur), each individual crisis having probability ω of escalating to war. As a result, the probability of no war over C crises is $(1 - \omega)^C$ (by Kolmogorov's theorem), so a country's epochal probability of war is given by

$$W = 1 - (1 - \omega)^C \tag{13}$$

which is a bivariate nonlinear hybrid function, where ω is continuous over the closed unit probability interval $[0, 1]$ and $C \geq 2$ is discrete. The case when $C = 1$ (a single crisis during an entire epoch) is trivial, since $W(\omega, 1) = \omega$, as is easily shown.

The politically relevant domain is bound by $0 \leq \omega \leq 1$ and $2 \leq C \lessapprox 20$ (same as before, both equations being functions of compound events).

The 3D surface graph of $W(\omega, C)$ is in Figure 3a, which shows the probability of war rising rapidly to a maximal plateau as escalation probability ω and C increase. The contour plot in Figure 3b looks straight down, which highlights the broad plateau where war probability converges to 1, flanked by the steep north-south escarpment along the west edge as $\omega \rightarrow 0$.

Each variable increases W in a different way, as shown in Figures 3c through f. Calculating the partial derivative and partial difference of W with respect to ω and C, respectively:

$$\partial_\omega W = C(1-\omega)^{C-1} \quad \text{(for } \omega\text{'s effect on } W\text{, in Figures 3c and d)} \tag{14}$$

$$\Delta_c W = \omega(1-\omega)^C \quad \text{(for } C\text{'s effect on } W\text{, in Figures 3e and f).} \tag{15}$$

Changes in escalation probability ω and number of crises C have clearly different effects on epochal war probability W, although both functions are positively valued:

Congruent political effects. Change in either escalation probability ω or number of crises C has a direct effect on W, as shown by strictly positive values of the graphs of derivatives and differences in Figure 3c through f.

[6] While Wright formulated the high-level crisis-probability framework, Snyder completed it by providing the probabilistic causal mechanism (Suppes 1984) within the crisis branching process.

First- and second-order effects. Whereas the contour plot of $W(\omega, C)$ shows strictly concave isocontours (Figure 3b), contours of the derivative $\partial_\omega W$ (Figure 3d) also show a convex, mild spur protruding on the southwestern wall of the escarpment, near $p = 0.2$, a second-order effect in opposite direction to the previous case (Figure 1d) and, again, not apparent from the basic model (equation 13 and Figures 3a and b).
Second-order effects caused by changes in number of crises. The graphs of the change in E with respect to number of crises, $\Delta_c W$ (equation 14 and Figures 3e and f), show a pronounced spur along the north-south direction descending from a high value of W along low values of ω as C increases away from the minimal value of 2. All the isolines show mixed concavity and convexity, which is another second-order effect.
Geometrically opposite spurs. The mild C-grown spur shown by $\partial_\omega W$ in Figures 3c and d and the more pronounced ω-grown spur in $\Delta_c W$ in Figures 3e and f have a type of reflective symmetry: the former protrudes from the C boundary at low values of ω and C, while the latter extends from the ω-boundary from low values ($p \approx 0.2$) toward high values of C. Both features are indicative of nonlinear effects on war probability W caused by underlying changes in crisis escalation ω and number of crises C.

Having obtained some initial insights on the nature of war probability as a function of crisis dynamics, we now investigate the Wright-Snyder hybrid model through standardized variables not based on units and, therefore, enable direct comparisons of causal effects. In this case we shall proceed by obtaining and analyzing elasticities of W with respect to ω and C, as shown in Figure 4. Calculation of the point elasticity and the arc elasticity of W with respect to ω and C yields the following set of hybrid equations:

$$\eta_\omega W = \frac{C\omega(1-\omega)^{C-1}}{1-(1-\omega)^C} \qquad \text{(for } \omega\text{'s percentage effect on } W\text{, in Figures 4a and b)} \tag{16}$$

$$\eta_c W = C\omega\left(\frac{1}{1-(1-\omega)^C} - 1\right) \qquad \text{(for } C\text{'s percentage effect on } W\text{, in Figures 4c and d)} \tag{17}$$

Based on these equations we see again that these standardized effects on W are quite different from the absolute, unit-based effects uncovered earlier (equations 14 and 15 and associated figures). Recalling the meaning of elasticities, here, point elasticity stands for percentage change in the probability of war onset with respect to percentage change in crisis escalation probability ω, while arc elasticity is the percentage change in epochal war probability W with respect to percentage change in number of crises C during the epoch. In this case both elasticities are rather complicated rational hybrid functions, including denominators that are exponential in C (from the standardizing transformation), as shown in Figures 4a through d. While formal analysis is feasible, visual analytics of graphs reveal numerous interesting features.

Figures 4a and b both show that point elasticity is high (i.e., war probability is strongly affected by escalation probability) at low ω values and highest at lowest values of both ω and C (red levels of the escarpment). This means that the risk of war changes most when crises are few and escalation probability low. By

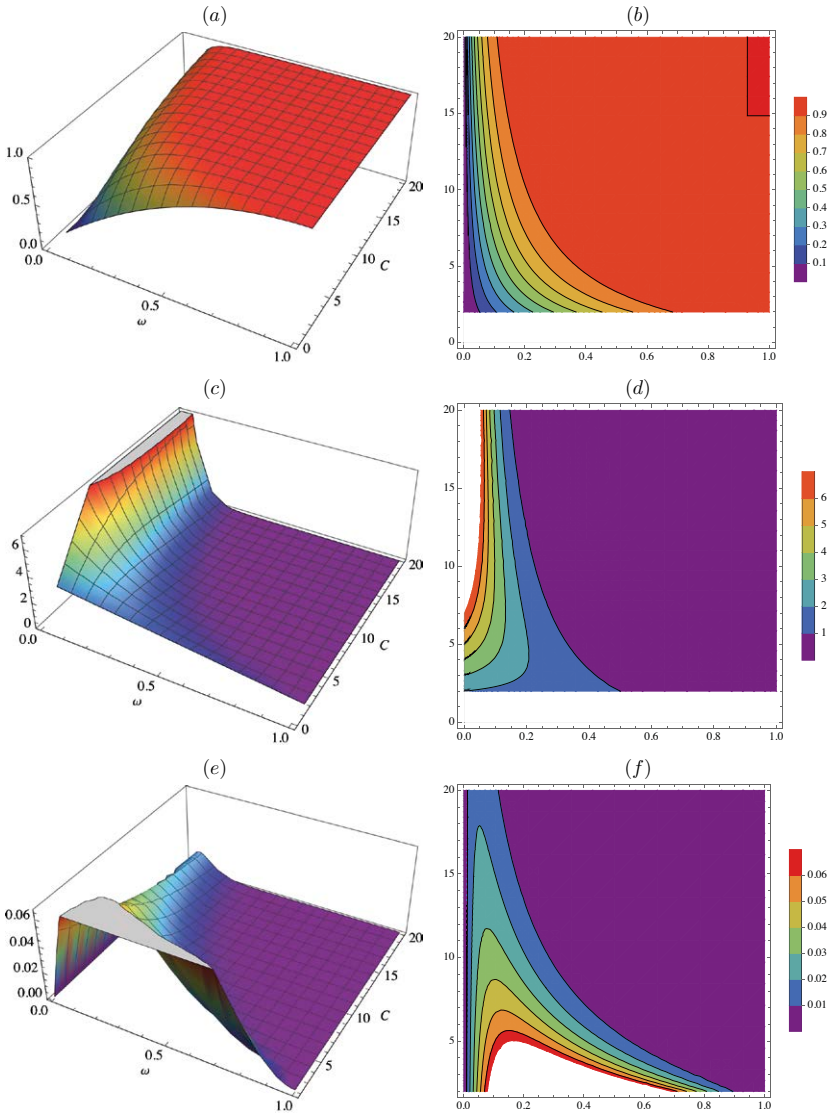

Figure 3. Epochal probability of war $W(\omega, C)$ as a hybrid function of crisis escalation probability ω and number of crises C: computational imagery from visualization analytics. (a) 3D surface of the hybrid function $W = (1 - \omega)^C$; (b) contour plot of (a); (c) 3D surface of $\partial_\omega W$, the first-order partial derivative of $W(\omega, C)$ with respect to ω; (d) contour plot of (c). (e) 3D surface of Δ_c, the first-order partial difference of $W(\omega, C)$ with respect to C; (f) contour plot of (e).

contrast, at the blue-green levels, war probability W is less sensitive to such instabilities (greater number of crises and higher escalation probability).

A rather subtle and surprising feature occurs along the front edge of the 3D surface in Figure 4, where point elasticity for all values of ω at the minimal boundary of $C = 2$ is convex (bulging up), whereas elsewhere (away from the front edge of the surface) point elasticity is strictly concave ($\partial\eta < 0$). This makes minimal epochs with only two crises rather special, which is not immediately intuitive. This particular property vanishes in all epochs with a multiplicity of crises beyond just two ($C \geq 3$). Concavity in point elasticity of W with respect to ω accelerates as the number of crises surpasses the first single digits.

By contrast, arc elasticity of war probability W is strictly concave, as seen in Figures 4c and d, convexity in this case being nonexistent (even at low C levels along the front edge).

Comparing the two elasticities (equations 16 and 17) yields the following dominance principle: epochal probability of war W is more sensitive to change in escalation probability ω than to change in number of crises C, because point elasticity η_ω is greater than arc elasticity η_c. The different but joint effects of escalation probability ω and number of crises C on epochal war probability W are analyzed and understood by calculating the gradient of W with respect to both variables using the nabladot operator, as follows:

$$\nabla W = \partial_\omega \left[1 - (1-\omega)^C\right] \mathbf{i} + \Delta_C \left[1 - (1-\omega)^C\right] \mathbf{j} \tag{18}$$

$$= C(1-\omega)^{C-1}\, \mathbf{i} + \omega(1-\omega)^C\, \mathbf{j}, \tag{19}$$

which is a two-dimensional vector function $\mathbf{W} = \mathbf{\Psi}(\omega, C)$. The resulting vector field of this hybrid gradient is in Figure 4e and corresponding vector magnitude or norm $|\mathbf{W}|(\omega, C)$, now a scalar function, is in Figure 4f.

We see from these results that both probability vector fields and norms $|\mathbf{W}|$ and $|\mathbf{E}|$, in Figures 2e and f and Figures 4e and f, resemble each other—a surprising result from comparative analysis—based on perfect bilateral vertical symmetries around the $P = \omega = 0.5$ axis. This is another political property not apparent from simple inspection of the basic models but consistent with formal fundamental symmetry and equivalence between causal logic conjunction and disjunction (De Morgan's laws) associated with the probability of international events (AND-based conjunctive) and epochal war probability (OR-based disjunctive), respectively.

4.3 Case 3: Frequency of war and systemic polarity (Midlarsky's law)

Having just examined the probability of war at the relational level, in this last case study we again change our frame of reference, this time turning to the systemic level of analysis. The formal theoretical (and empirically supported) explanation for the annual frequency of warfare as a result of fundamental po-

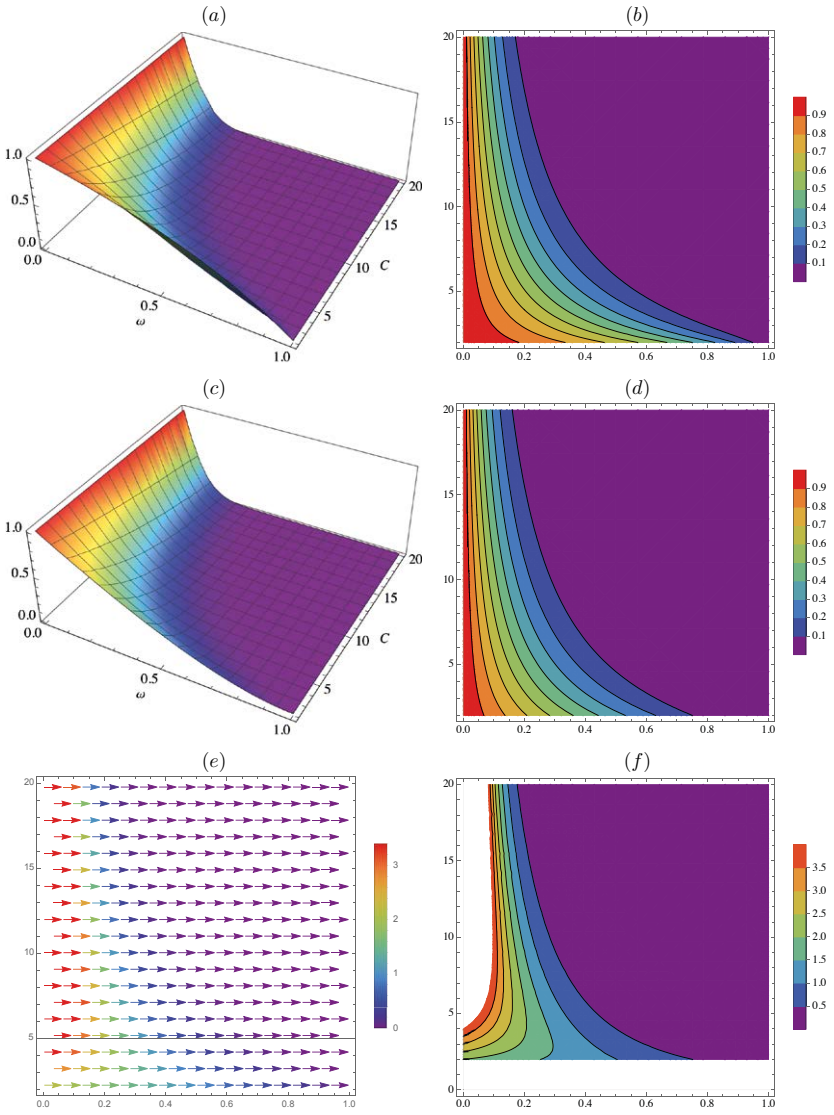

Figure 4. Elasticities and gradient of the epochal probability of war *W*. (a) 3D surface of point elasticity $\eta_{\omega}(W)$ with respect to crisis escalation probability ω; (b) contour plot of (a); (c) 3D surface of arc elasticity $\eta_{c}(W)$ with respect to epochal number of crises *C*; (d) contour plot of (c) ; (e) vector field of the dot-gradient vector function ∇W; (f) contour plot of (e).

litical uncertainty among great powers was pioneered by Manus I. Midlarsky in 1974. This causal theory is based on aspects of strategic uncertainty rooted in Shannon's information entropy and related concepts. The specific *explanandum* is the annual amount of warfare experienced in the international system, which is an emergent property generated not just by crises (as in the previous case) but also outright conquest, revenge, colonization, and all other types of wars. In any given year, Midlarsky's theory predicted that annual global war frequency ϕ is determined by systemic polarity Θ among the great powers.[7] Formally,

$$\phi = K \log \Theta, \tag{20}$$

which is a hybrid bivariate nonlinear function, where K is a continuous proportionality parameter over the closed interval $[1, 10]$, historically, and systemic polarity $\Theta \geq 1$ is discrete. The case when $\Theta = 1$ (a single hegemonic power) is the most peaceful, since $\phi(\Theta = 1) = 0$, and the function's (k, θ)-domain once again lies within Cartesian quadrant I.

The 3D surface graph of equation 20 is illustrated in Figure 5a, which shows war frequency rising on a hilly slope as polarity Θ and K increase. The associated contour plot in Figure 5b looks "straight down hill," highlighting the relatively mild gradient on the skirting slopes of the hybrid function, which is a surface bound by a linear slope along K but a logarithmically convex slope along Θ, a radial pattern observable in the plot's isocontours.

Each independent variable increases ϕ in a different way, as shown in Figures 5a and b. Calculating the partial derivative and partial difference of ϕ with respect to K and Θ, respectively:

$$\partial_k \phi = \ln \Theta \qquad \text{(for } K\text{'s effect on } W\text{, in Figure 5c)} \tag{21}$$

$$\Delta_\theta \phi = K\,[\ln(\Theta + 1) - \ln \Theta] \qquad \text{(for } \Theta\text{'s effect on } \phi\text{, in Figure 5e).} \tag{22}$$

Here, too, we see that changes in parameter K and polarity Θ have clearly different effects on war frequency ϕ, in this case through a simple univariate discrete function that is strictly discrete in Θ, and through a more complicated bivariate hybrid function (Figures 5c and d) with two terms in both dimensions, respectively.

Congruent political effects. Changes in parameter K or polarity Θ have proportional effects on ϕ, as shown by strictly positive values of both graphs of derivatives and differences in Figures 5c (2D) and e (3D), respectively. The graph of $\partial_k \phi$ lacks a contour plot, since it has univariate domain in Θ.

Isomorphism of ϕ and $\partial_k \phi$. War frequency ϕ and its rate of change with respect to K are isomorphic, as shown by Figure 5c and the estimated hybrid fun-

[7] Midlarsky's theory remains one of the most complete and empirically validated formal theories in international relations—and, surprisingly, one of the least known among conflict researchers. The initial validation based on 1815-1945 war onset data should not be retested on earlier and later datasets.

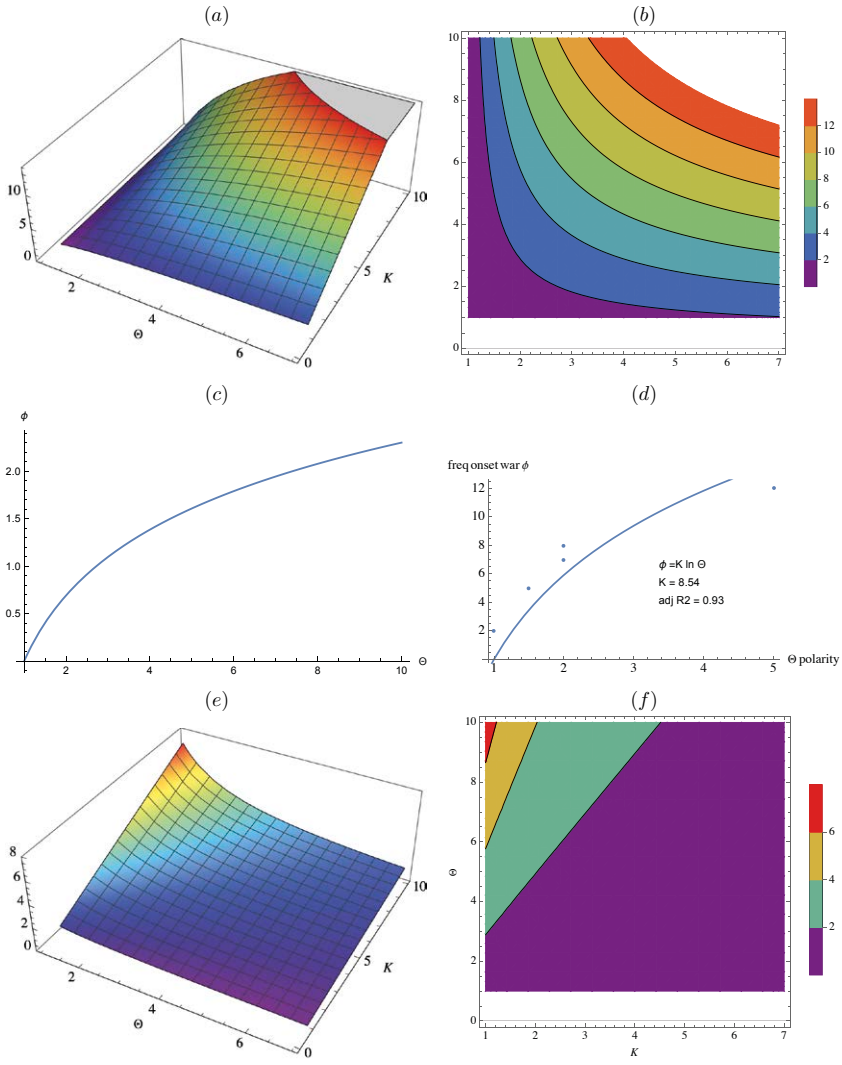

Figure 5. Annual frequency of war $\phi(K, \Theta)$ as a hybrid logarithmic function of systemic polarity Θ (Midlarsky's law): (a) 3D surface of the hybrid function $\phi = K \ln \Theta$; (b) contour plot of (a); (c) 2D graph of $\partial_k \phi$, the first-order partial derivative of ϕ with respect to K; (d) plot of the original function fitted on historical data constrained by the logarithmic condition $\phi(1) = 0$; (e) 3D surface of $\Delta_{\theta\phi}$ the first-order partial difference of ϕ with respect to Θ; (f) contour plot of (e).

ction $\hat{\phi}(K, \Theta)$ fitted to original data in Figure 5d (redrawn from Midlarsky 1974, 420, fig. 3).

Deceptive simplicity. Aside from the relatively simple convexity of war frequency ϕ induced by systemic polarity Θ, this theoretical model seems rather uncomplicated, as would appear from diagnostic images in Figure 5. However, such an impression may be superficial, as shown next by the second part of the analysis on elasticities and vector fields.

Finally, we can now investigate Midlarsky's law using standardized variables, as in the previous cases. First, we calculate and analyze percentage change in ϕ with respect to K and Θ, as shown by the elasticities in Figures 6a and b. Calculation of point elasticity and arc elasticity of ϕ with respect to parameter K and polarity Θ yields the following set of hybrid equations:

$$\eta_k \phi = 1 \qquad \text{(for } K\text{'s percentage effect on } \phi\text{, in Figure 6a)} \quad (23)$$

$$\eta_\theta \phi = \Theta \left[\frac{\ln(\Theta + 1)}{\ln \Theta} - 1 \right] \quad \text{(for } \Theta\text{'s percentage effect on } \phi\text{, in Figure 6b).} \quad (24)$$

We immediately see that standardized effects on ϕ are again quite different from earlier unit-based results (cf. equations 21 and 22 and associated figures). Here, point elasticity represents percentage change in annual war frequency with respect to percentage change in parameter K, whereas arc elasticity measures percentage change in ϕ with respect to percentage annual change in polarity Θ. The former has a constant value of 1 while the latter is a rational hybrid function with logarithms of polarity, as shown in Figures 6a and b, respectively.

Interestingly, arc elasticity (Figure 6b) exhibits a singularity under unipolarity, where $\phi(k, 1) = \infty$, indicating a major transition from unipolarity to bipolarity. In this case arc elasticity continues a rapid drop with increasing polarity, which is the systemic trend experienced in contemporary history of major powers after the Soviet-American Cold War around 1989.

Comparing the two elasticities (equations 23 and 24; cf. also their respective graphs in Figures 6a and b) yields the following dominance principle: annual frequency of war ϕ is more sensitive to percentage change in parameter K than to change in systemic polarity Θ under unipolar and bipolar systemic structures, but the reverse is true under tripolarity and higher-order structures—because the relationship reverses between $\Theta = 2$ and 3. This is a surprising qualitative transition that is invisible in the original model but is clear once the dimensions are standardized by elasticities.

The different and joint effects of parameter K and polarity Θ on war frequency ϕ can be seen by calculating the gradient of ϕ with respect to both variables using the nabladot operator, as follows:

$$\nabla \phi = \partial_k \left(K \ln \Theta \right) \mathbf{i} + \Delta_\theta \left(K \ln \Theta \right) \mathbf{j} \quad (25)$$

$$= \log \Theta \ \mathbf{i} + K \left[(\ln \Theta + 1) - \ln \Theta \right] \ \mathbf{j}, \quad (26)$$

which is a two-dimensional vector function $\mathbf{\Phi} = \mathbf{\Psi}(K, \Theta)$. The resulting vector field of this hybrid gradient is in Figure 6c, which shows: (i) heterogeneity along the two dimensions; (ii) general southwest-northeast orientation; (iii) increasing intensity as K increases for low values of polarity with a hot spot in the NW corner; (iv) divergence from a line at approximately 60 degrees; and (5) curling associated with divergence.

The corresponding vector magnitude or norm $|\mathbf{\Phi}|$, a scalar function, is shown by the contour plot in Figure 6d, on the same domain as the field. This shows other clear patterns, including a better view of (i) the hybrid gradient field $\mathbf{\Phi}$ that drops from the NW region into the uni- and bi-polar basin at minimal values of K—clearly where the most peaceful worlds are found—and (ii) a distinct view of the high ridge beyond $K \geq 5$ and $\Theta \geq 2$.

Given such marked differences between elasticity functions, it is best to investigate the standardized gradient, as follows:

$$\nabla^* \phi = \frac{K}{K \ln \Theta} \partial_k (K \ln \Theta)\, \mathbf{i} + \frac{\Theta}{K \ln \Theta} \Delta_\theta (K \ln \Theta)\, \mathbf{j} \tag{27}$$

$$= 1\mathbf{i} + \Theta \left[\frac{\ln(\Theta + 1)}{\ln \Theta} - 1 \right] \mathbf{j}, \tag{28}$$

which is a two-dimensional vector function $\mathbf{\Phi}^* = \mathbf{\Psi}^*(K, \Theta)$. The resulting vector field of this hybrid standardized gradient is seen in Figure 6e, which shows differences that are best highlighted by the corresponding 3D plot in Figure 6e. Here we see that the standardized gradient with respect to polarity undergoes a precipitous decline from unipolarity to bipolarity, after which it tapers off much more gradually and this feature is independent of K, consistent with elasticity results.

5. Conclusions

We began this chapter by observing that hybrid functions—formal models containing a combination of continuous and discrete variables—have been present in international relations theory since antiquity, *"hiding in plain sight,"* but their rigorous analysis has been impeded by the generally disjoint nature and established practices of infinitesimal calculus and discrete calculus. This problem has now been resolved by a unified approach that is feasible and fruitful, as provided by nabladot calculus.

Analysis of three separate cases in this chapter showed how and why, far from being intractable or only amenable to approximations, hybrid functions in international relations theory contain numerous interesting features and insightful properties that shed new light on our understanding of international phenomena. Nabladot analysis of each hybrid function—and subsequent comparative analysis across them—in each case revealed previously unknown and often scientifically surprising theoretical landscapes of international phenomena ranging from generic international events, to conditions of peace, crisis dynam-

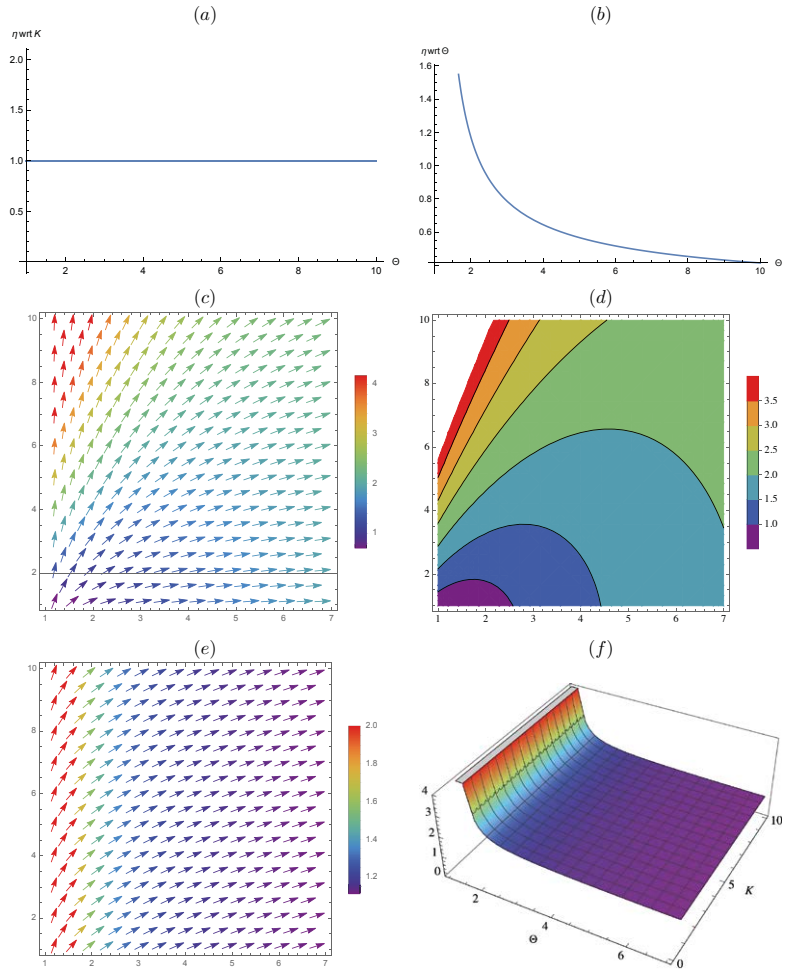

Figure 6. Elasticities and gradients of the annual frequency of war φ. (a) point elasticity $\eta_k(\phi)$ with respect to scale parameter K; (b) arc elasticity $\eta_\Theta(\phi)$ with respect to systemic polarity Θ; (c) vector field of the dot-gradient vector function $\nabla\phi$; (d) contour plot of (c). (e) vector field of the standardized dot-gradient vector function $\nabla\phi$; (f) 3D plot of (e).

ics, and warfare; all within the unified methods enabled by the hybrid nabladot operator and associated concepts, rather than through disjoint calculi or error-prone approximations.

These new theoretical landscapes and research frontiers are exciting and their application is still in a preliminary but already a demonstrably promising stage. Dominance principles that rank the influence of causal independent variables, singularities, previously undetected phase transitions, the deep nature of

probabilistic causality, and other scientifically intriguing results have intrinsic value for our understanding of international relations. As "progressive problem-shifts", in the sense of Lakatos (1973; cf. also Gillespie 1976 and Moore 2001), this novel and emergent corpus of scientific knowledge also provides rich and creative foundations for more advanced analyses that enhance our theoretical as well as practical understanding.

Acknowledgements

Grazie mille to professors Marco Cesa and Sonia Lucarelli for the kind invitation to contribute to this volume of papers in honor of my esteemed teacher and lifelong friend, Professor Umberto Gori. In retrospect, the earliest seeds of the nabladot calculus presented in this chapter were nucleated from my 1974 doctoral thesis, directed by Professor Gori at the University of Florence's *Scuola di Scienze Politiche e Sociali Cesare Alfieri*. Thanks to the Fenwick Library and the College of Science of George Mason University for use of the Mathematica system to create the figures and verify calculations. The editors and typographic staff of Florence University Press provided the excellent LaTeX template used to produce this chapter.

References

Ashford, Oliver M., H. Charnock, P. G. Drazin, J. C. R. Hunt, Paul Smoker, and Ian Sutherland, eds. 1993. *The Collected Papers of Lewis Fry Richardson, Volume 2: Quantitative Psychology and Studies of Conflict*. Cambridge, UK: Cambridge University Press.

Bittinger, Marvin L., and J. Conrad Crown. 1981. *Mathematics: a modeling approach*. Reading, Massachusetts: Addison-Wesley.

Boulding, Kenneth E. 1962. *Conflict and Defense: A General Theory*. New York: Harper and Row.

Bruschi, Alessandro. 1990. *Conoscenza e metodo: introduzione alla metodologia delle scienze sociali* [Knowledge and method: introduction to the methodology of the social sciences]. Milano: Edizioni Scolastiche Bruno Mondadori.

Cioffi-Revilla, Claudio. 1979. "Formal International Relations Theory: An Inventory, Review, and Integration." PhD diss., State University of New York at Buffalo. Proquest 7913870.

Cioffi-Revilla, Claudio. 1998. *Politics and uncertainty: theory, models and applications*. Cambridge, UK: Cambridge University Press.

Cioffi-Revilla Claudio. 2014. "Theoretical Nabladot Analysis of Amdahl's Law for Agent-Based Simulations." In *Euro-Par 2014: Parallel Processing Workshops*, edited by Lopes L. et al. Lecture Notes in Computer Science, vol. 8805, 440–51. Cham, Switzerland: Springer.

Cioffi-Revilla, Claudio. 2017. "On the exact calculus of hybrid functions." *Proceedings of the American Mathematical Society*, Southeastern Regional Meeting, University of Central Florida, Orlando, Florida, September 23, 2017.

Cioffi-Revilla, Claudio. 2019. "The nabladot operator for integrated calculus of hybrid functions with continuous and discrete variables." *Abstracts of Papers Presented to the American Mathematical Society* 40/1, 195 (Winter): 201.

Cioffi-Revilla, Claudio. 2020. "Hybrid Functions in the Sciences and Applied Mathematics." SSRN <https://ssrn.com/abstract=3579413> (aaaa-mm-gg). DOI:10.13140/RG.2.2.14376.11526

Cioffi-Revilla, Claudio. 2021. *Unified calculus of hybrid functions in the sciences and applied mathematics*. Monograph ms (in press).

Deutsch, Karl W. 1978[2]. *The Analysis of International Relations*. Englewood Cliffs, New Jersey: Prentice-Hall. Internet Archive: analysisofintern0000deut.

Eells, Ellery. 1991. *Probabilistic causality*. Vol. 1. Cambridge University Press.

Gillespie, John V. 1976. "Why mathematical models?" In *Mathematical Models in International Relations*, edited by Dina A. Zinnes and John V. Gillespie, 37–61. New York: Praeger.

Goertz, Gary, and Harvey Starr, eds. 2003. *Necessary Conditions*. Lanham, Maryland: Rowman & Littlefield.

Gori, Umberto. 2004. *Lezioni di Relazioni Internazionali*. Padova: Cedam.

Horvath, William J., and Caxton C. Foster. 1963. "Stochastic models of war alliances." *Journal of Conflict Resolution* 7 (2): 110–16.

Kline, Morris. 1985. *Mathematics and the Search for Knowledge*. Oxford-New York: Oxford University Press.

Kolmogorov, Andrey. 1933. *Grundbegriffe der Wahrscheinlichkeitsrechnung* (in German). Berlin: Julius Springer. Translation: Kolmogorov, Andrey. 1956[2]. *Foundations of the Theory of Probability*. New York: Chelsea.

Midlarsky, Manus I. 1974. "Power, uncertainty, and the onset of international violence." *Journal of Conflict Resolution* 18 (2): 395–431.

Moore, Will H. 2001. "Evaluating Theory in Political Science." Department of Political Science, The Florida State University, Tallahassee, Florida. August 9, 2001. Unpublished paper available online at: <https://whmooredotnet.files.wordpress.com/2014/07/evaluating-theory.pdf> (2001-08-09).

Moore, Will H., and David A. Siegel. 2013. *A Mathematics Course for Political and Social Research*. Princeton and Oxford: Princeton University Press.

Nicholson, Michael. 1989. *Formal Theories in International Relations*. New York: Cambridge University Press.

Salmon, Wesley C. 1980. "Probabilistic Causality." *Pacific Philosophical Quarterly* 61, 2: 50–74.

Snyder, Glenn H., and Paul Diesing. 1977. *Conflict Among Nations: Bargaining, Decisionmaking, and System Structure in International Crises*. Princeton, N.J.: Princeton University Press.

Suppes, Patrick. 1984. *Probabilistic Metaphysics*. New York-Oxford: Basil Blackwell.

Taagepera, Rein. 1968. "Growth curves of empires." *General Systems: Yearbook of the Society for General Systems Research* 13: 171–75.

Taagepera, Rein. 1978. "Size and duration of empires: growth-decline curves, 3000 to 600 BC." *Social Science Research* 7 (1): 180–96.

Taagepera, Rein. 1979. "Size and duration of empires: Growth-decline curves, 600 B.C. to 600 A.D." *Social Science History* 3: 115–38.

Thomas, James J., and Kristin A. Cook, eds. 2005. *Illuminating the Path*. Los Alamitos, California: IEEE Computer Society.

Wellin, Paul. 2013. *Programming with Mathematica*. Cambridge, UK: Cambridge University Press.

Wohlstetter, Albert. 1959. "The delicate balance of terror." *Foreign Affairs* 37 (1): 211–34.

Wohlstetter, Albert. 1968. "Theory and opposed-systems design." *Journal of Conflict Resolution* 12 (3): 302–31.

Wright, Quincy. 1942. *A Study of War, Vol. II*. Chicago: University of Chicago Press.